Nonlinear Dyn (2010) 61: 163–182
DOI 10.1007/s11071-009-9639-0

ORIGINAL PAPER

Internal-external resonance of beams on non-linear viscoelastic foundation traversed by moving load

M. Ansari · E. Esmailzadeh · D. Younesian

Received: 6 December 2009 / Accepted: 7 December 2009 / Published online: 23 January 2010

Abstract Vibration of a finite Euler–Bernoulli beam, supported by non-linear viscoelastic foundation traversed by a moving load, is studied and the Galerkin method is used to discretize the non-linear partial differential equation of motion. Subsequently, the solution is obtained for different harmonics using the Multiple Scales Method (MSM) as one of the perturbation techniques. Free vibration of a beam on non-linear foundation is investigated and the effects of damping and non-linear stiffness of the foundation on the responses are examined. Internal-external resonance condition is then stated and the frequency responses of different harmonics are obtained by MSM. Different conditions of the external resonance are studied and a parametric study is carried out for each case. The effects of damping and non-linear stiffness of the foundation as well as the magnitude of the moving load on the frequency responses are investigated. Finally, a thorough local stability analysis is performed on the system.

Keywords Non-linear vibration · Galerkin method · Moving load · Multiple scales method · Viscoelastic foundation · Perturbation method

M. Ansari · E. Esmailzadeh (✉) · D. Younesian
Faculty of Engineering and Applied Science, University of Ontario Institute of Technology, 2000 Simcoe St. North, Oshawa, Ontario, L1H 7K4, Canada
e-mail: ezadeh@uoit.ca

Present address:
M. Ansari
Department of Mechanical Engineering, University of Waterloo, Waterloo, Ontario, Canada

Present address:
D. Younesian
School of Railway Engineering, Iran University of Science & Technology, Tehran, Iran

1 Introduction

Vibration analysis of beams traversed by moving load is a well-known subject in structural mechanics and has also been of great interest by many engineers in different disciplines including mechanical, bridge, and railway engineering. Many researchers have conducted various investigations in the field of moving loads. Fryba [1] has presented fundamental studies in this area and cited more than 70 references in this area including most of the published articles before the turn of century.

Esmailzadeh and Ghorashi [2] studied the vibration of Timoshenko beams traversed by concentrated and partially distributed moving masses. They computed the beam response, and the distribution of the shear force and the bending moment along the beam, using the finite difference method. Andersen et al. [3] used the finite element method (FEM) to obtain the numerical solution of problems with external loads moving uniformly along an infinite Euler beam supported by a linear elastic Kelvin foundation with a linear viscous damping.

The vibration of a simply-supported beam traversed by uniform distributed moving loads was studied by Yu et al. [4]. They concluded that the dynamic response of the beam is tied up with these factors: the frequency of the beam, the moving frequency of the load and the ratio of the vehicle-beam mass. The dynamic analysis of bridges under moving loads was carried out by Gurav [5]. He implemented an orthotropic three-dimensional plate model to study the flexural and torsional properties of the bridge and also derived the eigen-value equations and normal mode shapes for an orthotropic plate.

Ouyang and Mottershead [6] investigated the vibration of a beam excited by a moving flexible body. They found that the deflection of the beam displays several cycles of oscillation during the passage of the moving body and can exceed the maximum static deflection at moderate speeds, but is close to the static deflection when the speed is either very low or very high. The study of vibration and dynamic buckling of shear beam-columns on elastic foundation under moving harmonic loads was carried out by Kim and Cho [7]. They examined as how the shear deformation of beams and the axial compression affect the local stability and vibration of systems and investigated the effects of various parameters, such as the load velocity, load frequency, shear rigidity, and the damping on the deflected shape, maximum displacement, and the critical values of the velocity, frequency, and the axial compression.

Martinez-Castro et al. [8] proposed a semi-analytic solution in the time domain for the non-uniform multi-span Euler–Bernoulli beams traversed by moving loads. In that research, the time-dependent modal equations are solved in closed-form and, therefore, the method is highly accurate and robust, circumventing the main disadvantages of time-stepping schemes. Garinei [9] focused on the vibrations of simple beam-like modeled bridge under harmonic moving loads. Ouyang and Mottershead [10] presented a combined numerical–analytical method for vibration of a beam excited by a moving flexible body. They discovered that the vibration of the moving body and the beam excited by the moving body are significantly influenced by the traveling speed, and the vibration levels tend to be greater in the intermediate speed range and the total moving force at the interface of the beam and the moving body can be compressive and tensile.

Stancioiu et al. [11] considered separation and reattachment in the study of the vibration of a beam excited by a moving oscillator. For any moving oscillator like the one being discussed in that paper, the stiffness of the spring connecting the two masses as well as the mass ratio can influence the onset of separation to a large extent. They concluded that it is more appropriate that for those studies, involving separation, the moving mass model should be replaced with the moving oscillator model, and when the spring stiffness becomes very high, the oscillator can usually be replaced with a single mass, without affecting the dynamic response of the beam. Kiral and Goren Kiral [12] focused on the dynamic behavior of a symmetrical laminated composite beam subjected to a concentrated force traveling at a constant velocity using a developed three-dimensional finite element model.

There are few works recently done on the study of non-linear vibrations of the beams subjected to either stationary or moving loads. Coskun and Engin [13] investigated the non-linear vibration of an elastic beam on a linear unstretched Winkler foundation subjected to a concentrated stationary load at its midpoint. They found that in contrast to the linear cases, the position of the lift-off points will change depending on the magnitude of the load and also, the vertical displacements change with the square of the load in the non-linear case; the dynamic effect in the linear case, the dynamic effect and the non-linearity arising from the foundation modulus in the non-linear case affect the variation of the contact lengths and the vertical displacements of the beam.

The non-linear dynamics of an Euler–Bernoulli beam under moving loads was studied by Yanmeni Wayou et al. [14] including the moving load inertia in the Duffing equation. They concluded that the load inertia can be neglected under two conditions:

(1) when the load velocity is higher than that leads to the resonance in the beam, and
(2) when the moving mass is very small compared to the mass of the beam.

Kang and Tan [15] conducted an investigation on non-linear response of a beam under distributed moving contact load. They applied a two-dimensional spectral balance method to solve the resulting extended Duffing's system, which is subjected to quasi-periodically modulated excitations.

For a beam resting on an elastic foundation, there are many cases in which, the foundation should be

considered non-linear for more appropriate investigations. Such systems have been treated by numerous researchers with diverse theoretical tools, including the numerical technique [16], finite element method [17–19], analytical approach [20–22] and the perturbation method [23]. In most of the published articles on the non-linear vibration of beams, subjected to moving loads, the non-linearity being of the geometrical type and arises from the large deformations of the beam.

There are very few published articles on the vibration of beams on non-linear foundations subjected to moving loads. Oscillations of a beam on non-linear elastic foundation under periodic fixed loads were studied by Santee and Goncalves [24] and the influence of a non-linear elastic foundation on the non-linear dynamic behavior and the local stability of slender beams were analyzed using a simplified model.

The problem of train-track interaction is one of the most important applications of such system in which, a railway track is resting on a viscoelastic ballast and traversed by a moving train. In most of the cited references discussed earlier, the foundation is assumed to be a linear mass-spring system with the view to simplify the model. Dahlberg [25] showed that the support structure of a railway track, in practice, is highly non-linear because of the hardening characteristic of the ballast. He solved the problem in the time domain and found that the differences between the results of the linear and non-linear models were quite considerable and deduced that a non-linear track model would represent the rail deflection fairly well.

Kargarnovin et al. [26] carried out a similar study in the frequency domain to find the response of infinite beams supported by non-linear viscoelastic foundations subjected to harmonic moving loads. They presented a straightforward solution technique applicable in the frequency domain.

The survey of the published research articles shows the lack of investigation on the subject of vibration of beams on non-linear foundations subjected to moving loads. That arises from two reasons, (a) the novelty of the concept of non-linearity of foundation that was verified experimentally in 2002 by Dahlberg [25], and (b) the complexity of the solution of the obtained non-linear partial differential equations of motion.

Abe [28] showed if discretizing the governing equation first by the use of the Galerkin method, then applying a shooting method to the obtained ordinary differential equations, and finally implementing the multiple scales method (MSM) [27], as being one of the perturbation methods, it will give more accurate results than when the multiple scales method is applied directly to the governing equation, which is a non-linear partial differential equation.

In this paper, the Galerkin method is utilized to discretize the governing equations and MSM perturbation method is applied to obtain the non-linear responses of the system. A railway track (finite beam) resting on ballast (non-linear viscoelastic foundation) traversed by a passing train (moving load) comprised the case study in this research. The Euler–Bernoulli beam theory is employed to model the finite beam and MSM is used to obtain the response of the free and forced vibration of the non-linear system. A comprehensive parametric sensitivity analysis is carried out to investigate the effects of different parameters on the dynamic performance of the system.

2 Problem formulation

The case of a uniform finite beam resting on non-linear viscoelastic foundation and subjected to a moving concentrated load is shown schematically in Fig. 1. Using the Hamilton principle and employing the Euler–Bernoulli theory, one can develop the governing differential equation of motion as

$$EIw_{xxxx} + kw + \alpha w^3 + \hat{\mu} w_t + \rho A w_{tt} = F_o \delta(x - vt) \tag{1}$$

where $E, I, A,$ and ρ are the respective modulus of elasticity, the second moment of area, the cross-sectional area of the beam, and the beam material density. The parameters k and α are the linear and non-linear parts of the foundation stiffness, $\hat{\mu}$ is the damping coefficient of the foundation, and F_o, v and w are the concentrated load, the moving load speed and the beam deflection, respectively.

It should be noted that since in reality, several foundations show non-linearities of the form of (1), the authors have chosen this type of model with the cubic non-linear term. In order to give a real sample of such non-linear behavior, one could consider the field

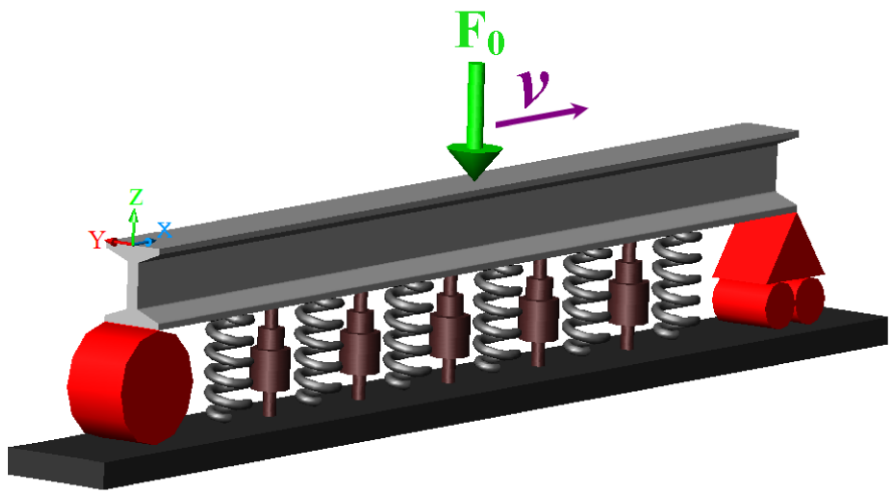

Fig. 1 A finite beam resting on a nonlinear viscoelastic foundation

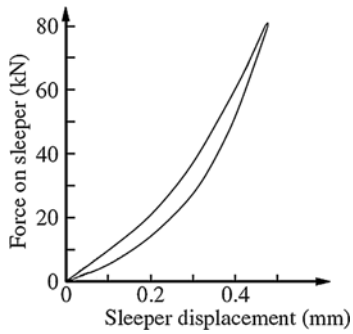

Fig. 2 Nonlinear behavior of a real case of railway track [29]

measurement results illustrated in Fig. 2. The detailed field measurement results can be found in [29]. An actual railway track was modeled by Dahlberg [25] using a hinge-hinge beam placed on a non-linear viscoelastic foundation and solved the dynamic problem in the time domain using FEM. He found that the differences in the results between the non-linear and linear models are considerable and a non-linear track model simulates the rail deflection quite well (compared with the measurements) whereas the equivalent linear model cannot as shown in Fig. 3. He validated his non-linear model experimentally within the frequency range of 0.1 to 20 Hz. Subsequently and in a more recent work, Wu and Thompson [30] used a similar non-linear model and studied the problem of wheel/track impact using the finite element method. They concluded that linear track models are not totally appropriate for the analysis of the wheel/track impact problems.

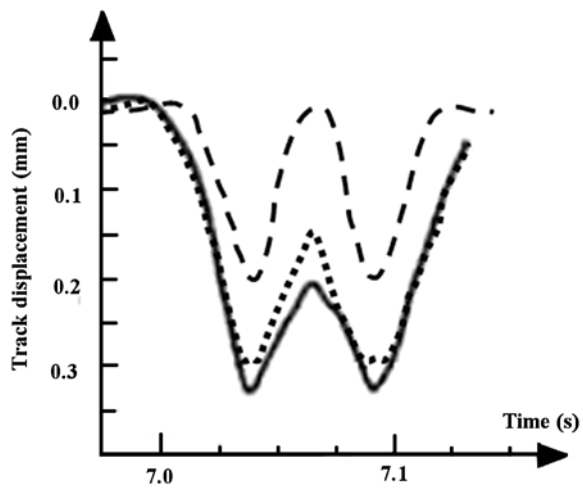

Fig. 3 Comparison between different models of railway track [25]. *Solid line* (—): field measurement; *dotted line* (. . .): nonlinear model; *dashed line* (– –): equivalent linear model

The beam is assumed simply supported at both ends with the boundary conditions:

$$w = w_{xx} = 0 \quad \text{at} \begin{cases} x = 0 \\ x = l \end{cases} \tag{2}$$

The Galerkin method is used to discretize the system with the following expansion in w

$$w = \sum_{n=1}^{\infty} u_n(t) \cdot \sin \frac{n\pi x}{l} \tag{3}$$

In general, it is convenient to assume the expansion of the displacement in terms of the linear free-oscillation modes. These functions and the natural

frequencies are intrinsic properties whereas, in the present research, the infinitesimal motions are well described by them. In order to find w, the first three terms of (3) were considered. Substituting (3) into (1) would lead to

$$\sum_{m=1}^{3}\left\{\left[\begin{array}{l}\rho A\ddot{u}_m(t)+\hat{\mu}\dot{u}_m(t)+\\ \left(\frac{m^4\pi^4 EI}{l^4}+k\right)u_m(t)\end{array}\right]\sin\left(\frac{m\pi x}{l}\right)\right\} + \alpha\left[\sum_{m=1}^{3}\left\{u_m(t)\cdot\sin\frac{m\pi x}{l}\right\}\right]^3 = F_o\delta(x-vt) \tag{4}$$

Using the orthogonality principle of the mode shapes and multiplying (4) by $\sin n\pi x/l$ and then integrating it over the interval length $[0, l]$ yields:

$$\ddot{u}_1+\omega_1^2u_1=-M\dot{u}_1-\alpha_1u_1^3-\alpha_2u_1^2u_3-\alpha_3u_1u_2^2-\alpha_4u_1u_3^2-\alpha_5u_2^2u_3+F_1\cos(\Omega_1t+\tau_1), \tag{5}$$

$$\ddot{u}_2+\omega_2^2u_2=-M\dot{u}_2-\alpha_6u_2^3-\alpha_7u_1^2u_2-\alpha_8u_2u_3^2-\alpha_9u_1u_2u_3+F_2\cos(\Omega_2t+\tau_2), \tag{6}$$

$$\ddot{u}_3+\omega_3^2u_3=-M\dot{u}_3-\alpha_{10}u_3^3-\alpha_{11}u_3u_1^2-\alpha_{12}u_2^2u_3-\alpha_{13}u_2^2u_1-\alpha_{14}u_1^3+F_3\cos(\Omega_3t+\tau_3) \tag{7}$$

where

$$\mu=\frac{1}{2}\frac{\hat{\mu}}{\rho A},\quad \Omega_1=\frac{1}{2}\Omega_2=\frac{1}{3}\Omega_3=\frac{\pi v}{l},$$

$$\alpha_1=\alpha_5=\alpha_6=\alpha_{10}=\alpha_{13}=\frac{3}{4}\frac{\alpha}{\rho A},$$

$$\alpha_3=\alpha_4=\alpha_7=\alpha_8=\alpha_9=\alpha_{11}=\alpha_{12}=\frac{3}{2}\frac{\alpha}{\rho A},$$

$$\alpha_2=-\frac{3}{4}\frac{\alpha}{\rho A},\quad \alpha_{14}=-\frac{1}{4}\frac{\alpha}{\rho A},$$

$$\omega_1^2=\frac{EI\pi^4}{\rho Al^4}+\frac{k}{\rho A},\quad \omega_2^2=\frac{16EI\pi^4}{\rho Al^4}+\frac{k}{\rho A},$$

$$\omega_3^2=\frac{81EI\pi^4}{\rho Al^4}+\frac{k}{\rho A},$$

$$F_1=\varepsilon^3f_1,\quad F_2=\varepsilon^3f_2,\quad F_3=\varepsilon^3f_3,\quad M=\varepsilon^2\mu$$

and $\tau_1=\tau_2=\tau_3=-\frac{\pi}{2}$.

In these equations, ε is a considered as a small and the dimensionless parameter and the order of the amplitude, F_n and M are set in such a way that, in the case of the primary resonances, the effect of the damping term, non-linearity, and the excitation term appear in the same perturbation equations.

An asymptotic expansion would be in the form of

$$u_i=\varepsilon u_{i1}(T_o,T_2)+\varepsilon^3u_{i3}(T_o,T_2)+\cdots\quad \text{for } i=1 \text{ to } 3 \tag{8}$$

where $T_n=\varepsilon^nt$.

Since the non-linearity is in the form of cubic, the terms $O(\varepsilon^2)$and the scale T_1 are missing from (8). By substituting (8) into (5), (6), and (7) and equating the coefficients of the same powers of ε, one could obtain

Order ε:

$$D_o^2u_{i1}+\omega_i^2u_{i1}=0\quad \text{for } i=1 \text{ to } 3 \tag{9}$$

Order ε^3:

$$D_o^2u_{13}+\omega_1^2u_{13}=-2D_oD_2u_{11}-2\mu D_ou_{11}-\alpha_1u_{11}^3-\alpha_2u_{11}^2u_{31}-\alpha_3u_{11}u_{21}^2-\alpha_4u_{11}u_{31}^2-\alpha_5u_{21}^2u_{31}+f_1\cos(\Omega t+\tau_1), \tag{10}$$

$$D_o^2u_{23}+\omega_2^2u_{23}=-2D_oD_2u_{21}-2\mu D_ou_{21}-\alpha_6u_{21}^3-\alpha_7u_{11}^2u_{21}-\alpha_8u_{21}u_{31}^2-\alpha_9u_{11}u_{21}u_{31}+f_2\cos(2\Omega t+\tau_2), \tag{11}$$

$$D_o^2u_{33}+\omega_3^2u_{33}=-2D_oD_2u_{31}-2\mu D_ou_{31}-\alpha_{10}u_{31}^3-\alpha_{11}u_{11}^2u_{31}-\alpha_{12}u_{31}u_{21}^2-\alpha_{13}u_{11}u_{21}^2-\alpha_{14}u_{11}^3+f_3\cos(3\Omega t+\tau_3) \tag{12}$$

The solutions of (9) can be expressed in the following form:

$$u_{i1}=A_i(T_2)\exp(i\omega_iT_o)+cc\quad \text{for } i=1 \text{ to } 3 \tag{13}$$

where cc denotes the complex conjugate of the preceding terms.

Substituting u_{i1} in (10), (11), and (12) one can obtain the following equations:

$$
\begin{aligned}
&D_o^2 u_{13} + \omega_1^2 u_{13} \\
&\quad = -2\alpha_4 A_1 A_3 \bar{A}_3 \exp(i\omega_1 T_o) \\
&\qquad - 2\alpha_3 A_1 A_2 \bar{A}_2 \exp(i\omega_1 T_o) \\
&\qquad - 2i\mu\omega_1 A_1 \exp(i\omega_1 T_o) - 2i A_1' \omega_1 \exp(i\omega_1 T_o) \\
&\qquad - 3\alpha_1 A_1^2 \bar{A}_1 \exp(i\omega_1 T_o) \\
&\qquad - \alpha_2 \bar{A}_1^2 A_3 \exp[i(\omega_3 - 2\omega_1)T_o] \\
&\qquad - \alpha_4 A_1 A_3^2 \exp[i(\omega_1 + 2\omega_3)T_o] \\
&\qquad - \alpha_5 A_2^2 \bar{A}_3 \exp[i(2\omega_2 - \omega_3)T_o] \\
&\qquad - 2\alpha_5 A_2 \bar{A}_2 A_3 \cdot \exp(i\omega_3 T_o) \\
&\qquad - \alpha_5 A_2^2 A_3 \exp[i(2\omega_2 + \omega_3)T_o] \\
&\qquad - \alpha_4 A_1 \bar{A}_3^2 \exp[i(\omega_1 - 2\omega_3)T_o] \\
&\qquad - \alpha_3 A_1 \bar{A}_2^2 \exp[i(\omega_1 - 2\omega_2)T_o] \\
&\qquad - \alpha_2 A_1^2 A_3 \exp[i(2\omega_1 + \omega_3)T_o] \\
&\qquad - 2\alpha_2 A_1 \bar{A}_1 A_3 \cdot \exp(i\omega_3 T_o) \\
&\qquad - \alpha_3 A_1 A_2^2 \exp[i(\omega_1 + 2\omega_2)T_o] \\
&\qquad - \alpha_1 A_1^3 \exp(3i\omega_1 T_o) \\
&\qquad + \frac{1}{2} f_1 \exp[i(\Omega_1 T_o + \tau_1)] + cc, \qquad (14)
\end{aligned}
$$

$$
\begin{aligned}
&D_o^2 u_{23} + \omega_2^2 u_{23} \\
&\quad = -3\alpha_6 A_2^2 \bar{A}_2 \exp(i\omega_2 T_o) \\
&\qquad - 2\alpha_7 A_2 A_1 \bar{A}_1 \exp(i\omega_2 T_o) \\
&\qquad - 2\alpha_8 A_2 A_3 \bar{A}_3 \exp(i\omega_2 T_o) \\
&\qquad - 2i\mu A_2 \omega_2 \exp(i\omega_2 T_o) \\
&\qquad - 2i A_2' \omega_2 \exp(i\omega_2 T_o) - \alpha_6 A_2^3 \exp(3i\omega_2 T_o) \\
&\qquad - \alpha_9 \bar{A}_1 A_2 \bar{A}_3 \exp[i(\omega_2 - \omega_1 - \omega_3)T_o] \\
&\qquad - \alpha_9 \bar{A}_1 A_2 A_3 \exp[i(\omega_2 + \omega_3 - \omega_1)T_o] \\
&\qquad - \alpha_9 A_1 A_2 \bar{A}_3 \exp[i(\omega_1 + \omega_2 - \omega_3)T_o] \\
&\qquad - \alpha_9 A_1 A_2 A_3 \exp[i(\omega_1 + \omega_2 + \omega_3)T_o] \\
&\qquad - \alpha_7 A_2 \bar{A}_1^2 \exp[i(\omega_2 - 2\omega_1)T_o] \\
&\qquad - \alpha_7 A_2 A_1^2 \exp[i(\omega_2 + 2\omega_1)T_o] \\
&\qquad - \alpha_8 A_2 A_3^2 \cdot \exp[i(\omega_2 + 2\omega_3)T_o] \\
&\qquad - \alpha_8 A_2 \bar{A}_3 \exp[i(\omega_2 - 2\omega_3)T_o] \\
&\qquad + \frac{1}{2} f_2 \exp[i(\Omega_2 T_o + \tau_2)] + cc, \qquad (15)
\end{aligned}
$$

$$
\begin{aligned}
&D_o^2 u_{33} + \omega_3^2 u_{33} \\
&\quad = -3\alpha_{10} A_3^2 \bar{A}_3 \exp(i\omega_3 T_o) - \alpha_{14} A_1^3 \exp(3i\omega_1 T_o) \\
&\qquad - 2\alpha_{11} A_1 \bar{A}_1 A_3 \exp(i\omega_3 T_o) \\
&\qquad - 2\alpha_{12} A_2 \bar{A}_2 A_3 \exp(i\omega_3 T_o) \\
&\qquad - 2i A_3' \omega_3 \exp(i\omega_3 T_o) - 2i\mu A_3 \omega_3 \exp(i\omega_3 T_o) \\
&\qquad - \alpha_{10} A_3^3 \exp(3i\omega_3 T_o) \\
&\qquad - \alpha_{11} A_1^2 A_3 \exp[i(2\omega_1 + \omega_3)T_o] \\
&\qquad - \alpha_{11} \bar{A}_1^2 A_3 \cdot \exp[i(\omega_3 - 2\omega_1)T_o] \\
&\qquad - \alpha_{12} A_2^2 A_3 \exp[i(2\omega_2 + \omega_3)T_o] \\
&\qquad - \alpha_{12} \bar{A}_2^2 A_3 \cdot \exp[i(\omega_3 - 2\omega_2)T_o] \\
&\qquad - \alpha_{13} \bar{A}_1 A_2^2 \exp[i(2\omega_2 - \omega_1)T_o] \\
&\qquad - 2\alpha_{13} A_1 A_2 \bar{A}_2 \cdot \exp(i\omega_1 T_o) \\
&\qquad - 3\alpha_{14} A_1^2 \bar{A}_1 \exp(i\omega_1 T_o) \\
&\qquad - \alpha_{13} A_1 A_2^2 \exp[i(\omega_1 + 2\omega_2)T_o] \\
&\qquad + \frac{1}{2} f_3 \exp[i(\Omega_3 T_o + \tau_3)] + cc \qquad (16)
\end{aligned}
$$

2.1 Three-to-one internal resonance

The case of the internal resonance is of much interest and should be considered here in depth. The internal resonance would occur when

$$k = \frac{9EI\pi^4}{l^4} \Rightarrow \omega_3 = 3\omega_1 \qquad (17)$$

In order to quantitatively express the neighborhood of ω_3 to $3\omega_1$, a detuning parameter, σ, is defined so that $\omega_3 = 3\omega_1 + \varepsilon^2\sigma$

Therefore,

$$\omega_3 T_o = 3\omega_1 T_o + \varepsilon^2 \sigma T_o = 3\omega_1 T_o + \sigma T_2 \qquad (18)$$

To eliminate the terms that produce secular terms, one can state that the coefficients of $\exp(i\omega_1 T_o)$, $\exp(i\omega_2 T_o)$, and $\exp(i\omega_3 T_o)$ on the right-hand side of (14) to (16), respectively, should be set to zero.

Eliminating the secular terms would then lead to the following equations:

$$-2\alpha_4 A_1 A_3 \bar{A}_3 - 2\alpha_3 A_1 A_2 \bar{A}_2 - 2i\mu\omega_1 A_1 - 2i A_1'\omega_1 - 3\alpha_1 A_1^2 \bar{A}_1 - \alpha_2 \bar{A}_1^2 A_3 \exp(i\sigma T_2) = 0, \quad (19)$$

$$-3\alpha_6 A_2^2 \bar{A}_2 - 2\alpha_7 A_2 A_1 \bar{A}_1 - 2\alpha_8 A_2 A_3 \bar{A}_3 - 2i\mu A_2\omega_2 - 2i A_2'\omega_2 = 0, \quad (20)$$

$$-3\alpha_{10} A_3^2 \bar{A}_3 - \alpha_{14} A_1^3 \exp(-i\sigma T_2) - 2\alpha_{11} A_1 \bar{A}_1 A_3 - 2\alpha_{12} A_2 \bar{A}_2 A_3 - 2i A_3'\omega_3 - 2i\mu A_3\omega_3 = 0 \quad (21)$$

Eliminating the terms which, produce the secular terms in these equations and substituting the polar coordinates notation, in the form of (22), into the obtained equations and by separating the real and the imaginary parts, one could obtain

$$A_m = \frac{1}{2} a_m \exp(i\theta_m) \quad \text{for } m = 1 \text{ to } 3, \quad (22)$$

$$a_1\omega_1\theta_1' - \frac{3}{8}\alpha_1 a_1^3 - \frac{1}{4}\alpha_4 a_1 a_2^2 - \frac{1}{4}\alpha_4 a_1 a_3^2 - \frac{1}{8}\alpha_2 a_1^2 a_3 \cos\gamma = 0, \quad (23)$$

$$-\omega_1 a_1' - \mu a_1\omega_1 - \frac{1}{8}\alpha_2 a_1^2 a_3 \sin\gamma = 0, \quad (24)$$

$$-\frac{1}{4}\alpha_7 a_2 a_1^2 - \frac{1}{4}\alpha_8 a_2 a_3^2 + \omega_2\theta_2' a_2 - \frac{3}{8}\alpha_6 a_2^3 = 0, \quad (25)$$

$$-\mu a_2\omega_2 - a_2'\omega_2 = 0, \quad (26)$$

$$-\frac{1}{4}\alpha_{12} a_2^2 a_3 - \frac{3}{8}\alpha_{10} a_3^3 + \theta_3'\omega_3 a_3 - \frac{1}{4}\alpha_{11} a_1^2 a_3 - \frac{1}{8}\alpha_{14} a_1^3 \cos\gamma = 0, \quad (27)$$

$$-\omega_3 a_3' - \mu a_3\omega_3 + \frac{1}{8}\alpha_{14} a_1^3 \sin\gamma = 0, \quad (28)$$

where $\gamma = \sigma T_2 + \theta_3 - 3\theta_1$.

2.2 Forced vibration

With regards to (14), (15), and (16), an internal resonance should occur when $\omega_3 \approx 3\omega_1$. Hence, a similar detuning parameter σ_1 must be defined:

$$\omega_3 = 3\omega_1 + \varepsilon^2\sigma_1 \quad (29)$$

Now there are three possible cases that might occur.

2.2.1 Case 1 when $\Omega_1 \approx \omega_1$

A new detuning parameter σ_2 should now be introduced in accordance with:

$$\Omega_1 = \omega_1 + \varepsilon^2\sigma_2 \quad (30)$$

By substituting (29) and (30) into (14), (15), and (16), one could obtain the solvability condition of the system. Using (22) and by separating the real and the imaginary parts, and eliminating the secular terms, one could obtain

$$a_1\omega_1\theta_1' - \frac{3}{8}\alpha_1 a_1^3 - \frac{1}{4}\alpha_4 a_1 a_2^2 - \frac{1}{4}\alpha_4 a_1 a_3^2 - \frac{1}{8}\alpha_2 a_1^2 a_3 \cos\gamma_1 + \frac{1}{2} f_1 \cos\gamma_2 = 0, \quad (31)$$

$$-\omega_1 a_1' - \mu a_1\omega_1 - \frac{1}{8}\alpha_2 a_1^2 a_3 \sin\gamma_1 + \frac{1}{2} f_1 \sin\gamma_2 = 0, \quad (32)$$

$$-\frac{1}{4}\alpha_7 a_2 a_1^2 - \frac{1}{4}\alpha_8 a_2 a_3^2 + \omega_2\theta_2' a_2 - \frac{3}{8}\alpha_6 a_2^3 = 0, \quad (33)$$

$$-\mu a_2\omega_2 - a_2'\omega_2 = 0, \quad (34)$$

$$-\frac{1}{4}\alpha_{12} a_2^2 a_3 - \frac{3}{8}\alpha_{10} a_3^3 + \theta_3'\omega_3 a_3 - \frac{1}{4}\alpha_{11} a_1^2 a_3 - \frac{1}{8}\alpha_{14} a_1^3 \cos\gamma_1 = 0, \quad (35)$$

$$-\omega_3 a_3' - \mu a_3\omega_3 + \frac{1}{8}\alpha_{14} a_1^3 \sin\gamma_1 = 0, \quad (36)$$

where $\gamma_1 = \sigma_1 T_2 + \theta_3 - 3\theta_1$ and $\gamma_2 = \sigma_2 T_2 - \theta_1 + \tau_1$.

2.2.2 Case 2 when $\Omega_2 \approx \omega_2$

In this case, following the same procedure as mentioned in Sect. 2.2.1 with different detuning parameter, one could determine the following equations, which must also be satisfied in order for that the secular terms be eliminated.

$$a_1\omega_1\theta_1' - \frac{3}{8}\alpha_1 a_1^3 - \frac{1}{4}\alpha_4 a_1 a_2^2 - \frac{1}{4}\alpha_4 a_1 a_3^2 - \frac{1}{8}\alpha_2 a_1^2 a_3 \cos\gamma_1 = 0, \quad (37)$$

$$-\omega_1 a_1' - \mu a_1\omega_1 - \frac{1}{8}\alpha_2 a_1^2 a_3 \sin\gamma_1 = 0, \quad (38)$$

$$-\frac{1}{4}\alpha_7 a_2 a_1^2 - \frac{1}{4}\alpha_8 a_2 a_3^2 + \omega_2 \theta_2' a_2 - \frac{3}{8}\alpha_6 a_2^3 + \frac{1}{2} f_2 \cos\gamma_2 = 0, \tag{39}$$

$$-\mu a_2 \omega_2 - a_2' \omega_2 + \frac{1}{2} f_2 \sin\gamma_2 = 0, \tag{40}$$

$$-\frac{1}{4}\alpha_{12} a_2^2 a_3 - \frac{3}{8}\alpha_{10} a_3^3 + \theta_3' \omega_3 a_3 - \frac{1}{4}\alpha_{11} a_1^2 a_3 - \frac{1}{8}\alpha_{14} a_1^3 \cos\gamma_1 = 0, \tag{41}$$

$$-\omega_3 a_3' - \mu a_3 \omega_3 + \frac{1}{8}\alpha_{14} a_1^3 \sin\gamma_1 = 0, \tag{42}$$

where $\gamma_1 = \sigma_1 T_2 + \theta_3 - 3\theta_1$ and $\gamma_2 = \sigma_2 T_2 - \theta_2 + \tau_2$.

2.2.3 Case 3 when $\Omega_3 \approx \omega_3$

One could state that in this case, the following equations must be satisfied:

$$a_1 \omega_1 \theta_1' - \frac{3}{8}\alpha_1 a_1^3 - \frac{1}{4}\alpha_4 a_1 a_2^2 - \frac{1}{4}\alpha_4 a_1 a_3^2 - \frac{1}{8}\alpha_2 a_1^2 a_3 \cos\gamma_1 = 0, \tag{43}$$

$$-\omega_1 a_1' - \mu a_1 \omega_1 - \frac{1}{8}\alpha_2 a_1^2 a_3 \sin\gamma_1 = 0, \tag{44}$$

$$-\frac{1}{4}\alpha_7 a_2 a_1^2 - \frac{1}{4}\alpha_8 a_2 a_3^2 + \omega_2 \theta_2' a_2 - \frac{3}{8}\alpha_6 a_2^3 = 0, \tag{45}$$

$$-\mu a_2 \omega_2 - a_2' \omega_2 = 0, \tag{46}$$

$$-\frac{1}{4}\alpha_{12} a_2^2 a_3 - \frac{3}{8}\alpha_{10} a_3^3 + \theta_3' \omega_3 a_3 - \frac{1}{4}\alpha_{11} a_1^2 a_3 - \frac{1}{8}\alpha_{14} a_1^3 \cos\gamma_1 + \frac{1}{2} f_3 \cos\gamma_2 = 0, \tag{47}$$

$$-\omega_3 a_3' - \mu a_3 \omega_3 + \frac{1}{8}\alpha_{14} a_1^3 \sin\gamma_1 + \frac{1}{2} f_3 \sin\gamma_2 = 0, \tag{48}$$

where $\gamma_1 = \sigma_1 T_2 + \theta_3 - 3\theta_1$ and $\gamma_2 = \sigma_2 T_2 - \theta_3 + \tau_3$.

3 Numerical results

To find the steady-state response in all those cases, which were mentioned in Sect. 2, the following conditions are implemented:

$$a_i' = \gamma_i' = 0 \tag{49}$$

Table 1 Geometrical and mechanical properties of the finite beam, non-linear foundation and the moving load [16]

Item	Notation	Value
Beam		
Length	l	18 m
Young's modulus (steel)	E	210 GPa
Mass density	ρ	7850 kg/m^3
Cross-sectional area	A	7.69×10^{-3} m^2
Second moment of area	I	30.55×10^{-6} m^4
Foundation		
Linear stiffness	k	35 MN/m^2
Non-linear stiffness	α	4×10^8 MN/m^4
Viscous damping	$\hat{\mu}$	1732.5 N s/m^2
Moving load		
Load	F_o	65 kN

A computer program is developed using MATLAB©, which was linked with the MAPLE© software to solve the equations numerically. The physical and geometrical properties of the finite beam and those of the non-linear foundation and the data for the moving load are listed in Table 1 [16].

Local stability analysis is performed on the system by linearization of (31) to (36) for Case 1, (37) to (42) for Case 2, and (43) to (48) for Case 3 for the parameters a_1, a_2, a_3, γ_1, and γ_2 around the singular (or the steady-state) points. In doing so, a set of linear equations with constant coefficients, multiplied by an unknown disturbance term, would be obtained and the eigen-value problem should then be formed. If the real part of every eigen-value of the coefficient matrix is positive then the point is unstable, otherwise must be stable.

After evaluating the values of the parameters a_1, a_2, a_3, γ_1, and γ_2, it would be assumed that each one is comprised of two parts: (i) a steady-state part, and (ii) a disturbance part. Therefore, one could write

$$a_1 = a_{1s} + a_{1d}, \quad a_2 = a_{2s} + a_{2d}, \quad a_3 = a_{3s} + a_{3d}, \quad \gamma_1 = \gamma_{1s} + \gamma_{1d}, \quad \text{and} \quad \gamma_2 = \gamma_{2s} + \gamma_{2d}$$

where a_{1s}, a_{2s}, a_{3s}, γ_{1s}, and γ_{2s} are the singular points and a_{1d}, a_{2d}, a_{3d}, γ_{1d}, and γ_{2d} are the disturbance parts of a_1, a_2, a_3, γ_1, and γ_2, respectively.

In order to define the nature of all the various singular points, the new forms of a_1, a_2, a_3, γ_1, and γ_2 with their derivatives are substituted into (31) to (36) for Case 1, (37) to (42) for Case 2, and (43) to (48) for Case 3. By expanding these relationships, one could solve the state-space equation $\{\dot{X}\} = [\mathbf{A}]\{X\}$ in order to obtain the eigen-values, where the matrix [**A**] is referred to the Jacobian matrix. By knowing the eigen-values, one could easily check the local stability of the system and in order to illustrate the unstable regions on the response graphs these have been indicated by the dashed lines in every figure.

It should be noted that the preceding analysis determines the linear or local stability of the steady-state solutions. The stability of motions in the large domain can be determined theoretically by the use of techniques applicable in the global stability analysis, e.g., the Lyapunov method. The other notable issue is that, within the practical range of engineering input parameters, no neutrally stable points were found along the points on the frequency response curves. In other words, no bifurcation points were recognized along the frequency-response curve and all the points were found to be either stable or unstable points. More explanations on this, including some case studies, are presented in the Appendix.

3.1 Free vibration

In considering the system response at the steady-state condition with (26), one can conclude that

$$a_2 = 0$$

and

$$a_3\gamma' = a_3\sigma + \left(\frac{3}{8}\frac{\alpha_{10}}{\omega_3} - \frac{3}{4}\frac{\alpha_4}{\omega_1}\right)a_3^2 + \left(\frac{1}{4}\frac{\alpha_{11}}{\omega_3} - \frac{9}{8}\frac{\alpha_1}{\omega_1}\right)a_1^2 a_3 + \left(\frac{1}{8}\frac{\alpha_{14}}{\omega_3}a_1^3 - \frac{3}{8}\frac{\alpha_2}{\omega_1}a_1 a_3^2\right)\cos\gamma \tag{50}$$

Furthermore, from (28), one could have

$$a_1' a_1 + \upsilon a_3' a_3 = -\mu a_1^2 - \mu\upsilon a_3^2 \tag{51}$$

where

$$\upsilon = \frac{\omega_3\alpha_2}{\omega_1\alpha_{14}}$$

Since α_2 and α_{14} have the same sign, therefore,

$$\upsilon > 0$$

For the steady-state motion one could write

$$a_1^2 + \upsilon a_3^2 = 0 \tag{52}$$

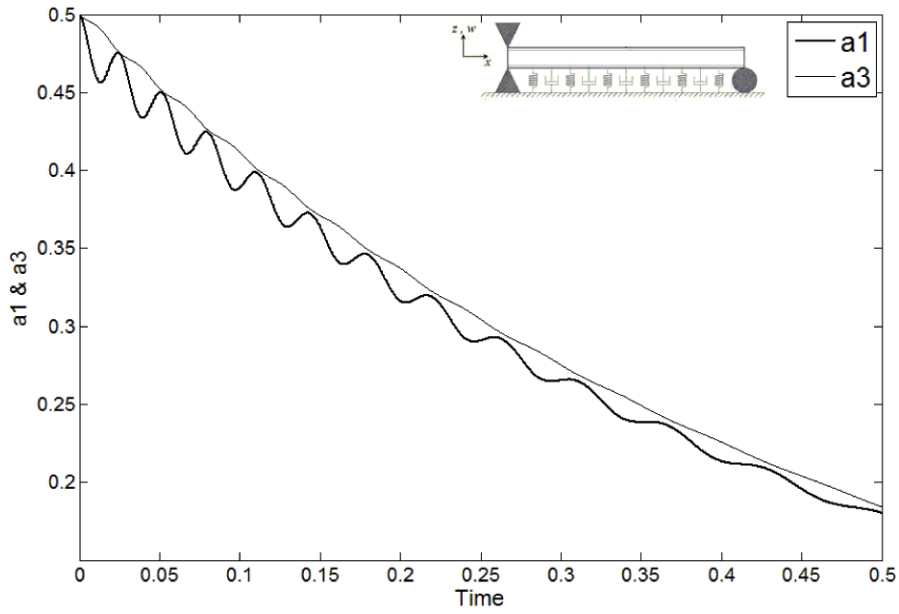

Fig. 4 Free oscillation amplitudes when $\omega_3 \approx 3\omega_1$

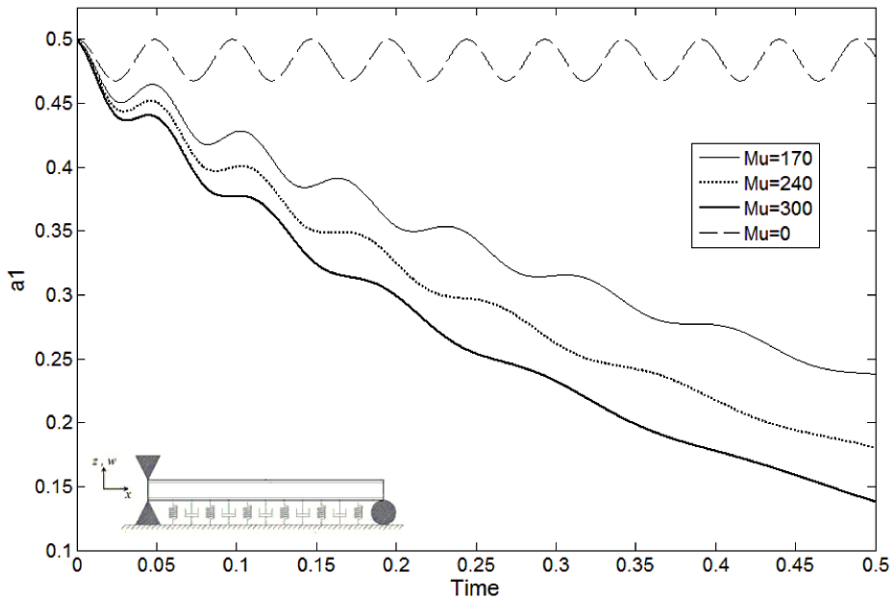

Fig. 5 Effects of damping coefficient on the free vibration of the system

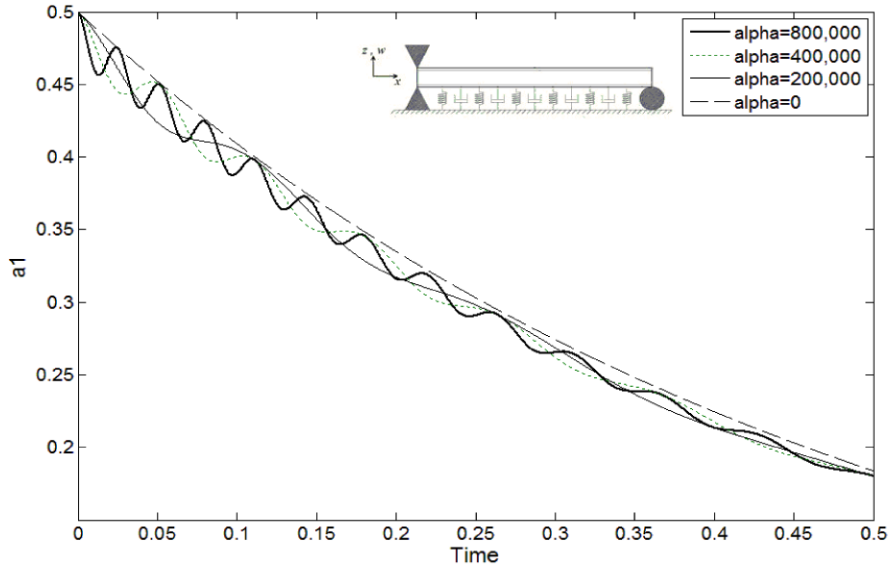

Fig. 6 Effects of nonlinear stiffness on the free vibration of the system

The integrated form of (51) is then obtained as

$$a_1^2 + \upsilon a_3^2 = E \cdot \exp(-2\varepsilon^2 \mu t) \tag{53}$$

where E is a constant of integration being proportional to the initial energy of the system.

One could conclude by saying that when $t \to \infty$, then $a_1^2 + \upsilon a_3^2 \to 0$, i.e., the energy present in the system decays exponentially with time. The variations of a_1 and a_3 with time, for the numerical solution of (24), (28), and (50), are illustrated in Fig. 4.

The effects of damping and non-linear stiffness on the free vibration of the system are presented in Figs. 5 and 6, respectively. It can be seen that the non-linear stiffness will increase the frequency of the vibration, but not the rate of the dissipation.

3.2 Forced vibration

The forced vibration analysis of the system under the condition of input excitation will be considered in this

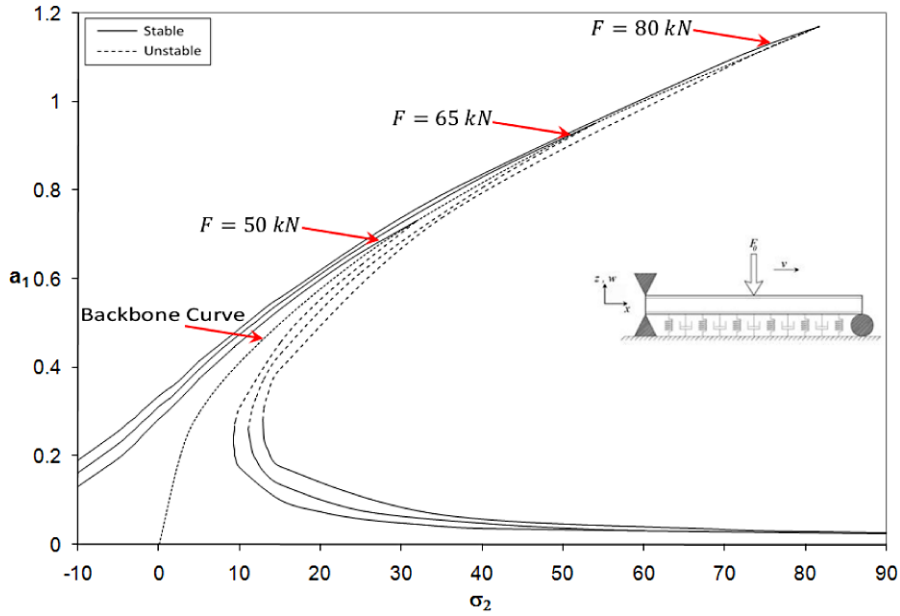

Fig. 7 (**a**) Frequency response curves for a_1 with $\omega_3 \approx 3\omega_1$, and $\Omega_1 \approx \omega_1$. (**b**) Frequency response curves for a_3 with $\omega_3 \approx 3\omega_1$, and $\Omega_1 \approx \omega_1$

section. The response of the system will be studied for different possible conditions.

3.2.1 Case (a) when $\Omega_1 \approx \omega_1$

In this case, by application of the steady-state response, (34) will lead to $\mu a_2 \omega_2 = 0$.

Since neither μ nor ω_2 are equal to zero, therefore,

$$a_2 = 0 \tag{54}$$

Taking the derivative of expression $\gamma_2 = \sigma_2 T_2 - \theta_1 + \tau_1$, one would obtain $\gamma_2' = \sigma_2 - \theta_1'$, which is rearranged as $\theta_1' = \sigma_2 - \gamma_2'$. Furthermore, by taking the derivative

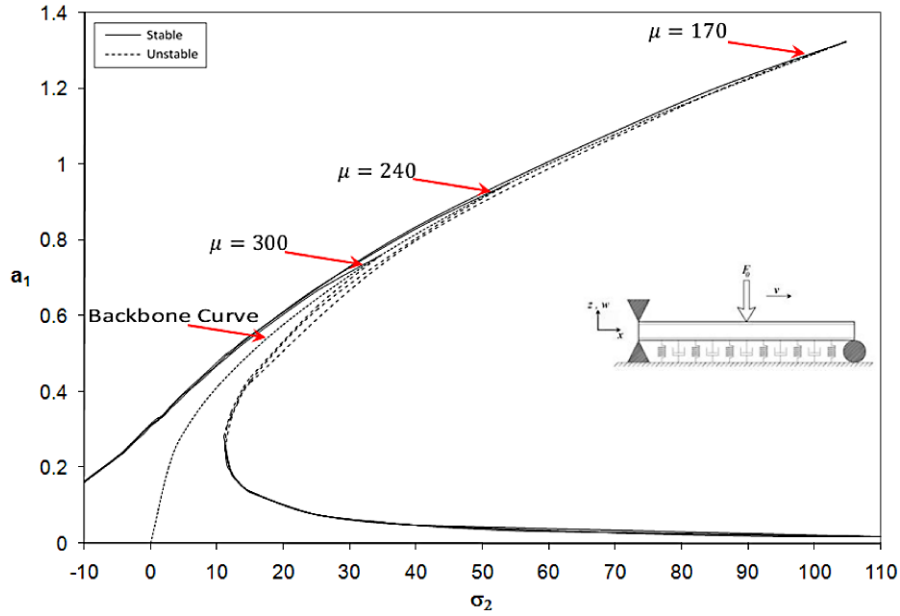

(a)

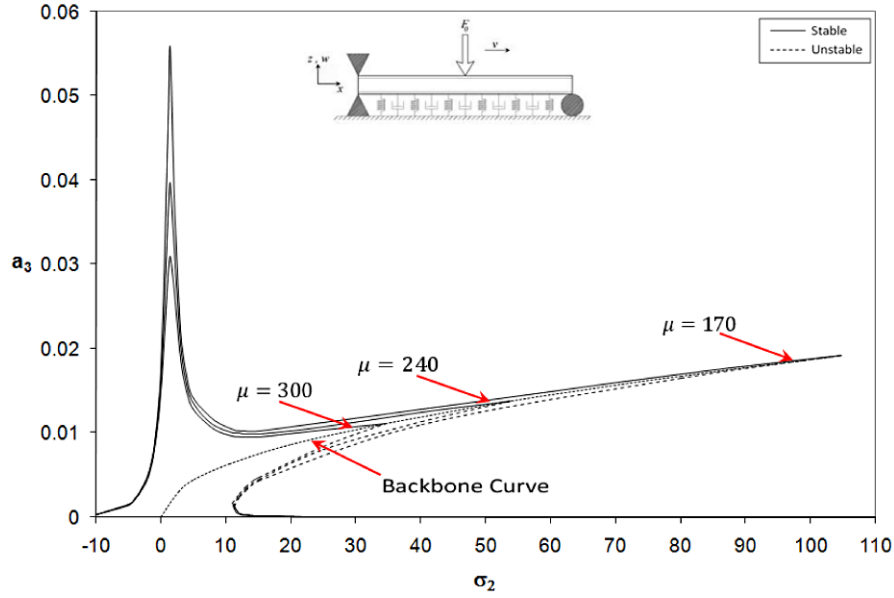

(b)

Fig. 8 (**a**) Effects of damping coefficient on frequency response for a_1 with $\omega_3 \approx 3\omega_1$, and $\Omega_1 \approx \omega_1$. (**b**) Effects of damping coefficient on frequency response for a_3 with $\omega_3 \approx 3\omega_1$, and $\Omega_1 \approx \omega_1$

of $\gamma_1 = \sigma_1 T_2 + \theta_3 - 3\theta_1$ one could arrive at $\gamma_1' = \sigma_1 + \theta_3' - 3\theta_1'$, which can be transformed into $\theta_3' = 3(\sigma_2 - \gamma_2') - \sigma_1 - \gamma_1'$. In the case of steady-state condition $\gamma_i' = 0$, hence $\theta_1' = \sigma_2$ and $\theta_3' = 3\sigma_2 - \sigma_1$.

By setting $a_2 = 0, \theta_1' = \sigma_2$ and $\theta_3' = 3\sigma_2 - \sigma_1$ and allowing $a_1' = a_2' = a_3' = 0$ in (31) through (36), one could obtain the following set of simultaneous equations, which must be solved for a_1, a_3, γ_1, and γ_2.

$$a_1\omega_1\sigma_2 - \frac{3}{8}\alpha_1 a_1^3 - \frac{1}{4}\alpha_4 a_1 a_3^2 - \frac{1}{8}\alpha_2 a_1^2 a_3 \cos\gamma_1 + \frac{1}{2} f_1 \cos\gamma_2 = 0, \tag{55}$$

$$-\mu a_1\omega_1 - \frac{1}{8}\alpha_2 a_1^2 a_3 \sin\gamma_1 + \frac{1}{2} f_1 \sin\gamma_2 = 0, \tag{56}$$

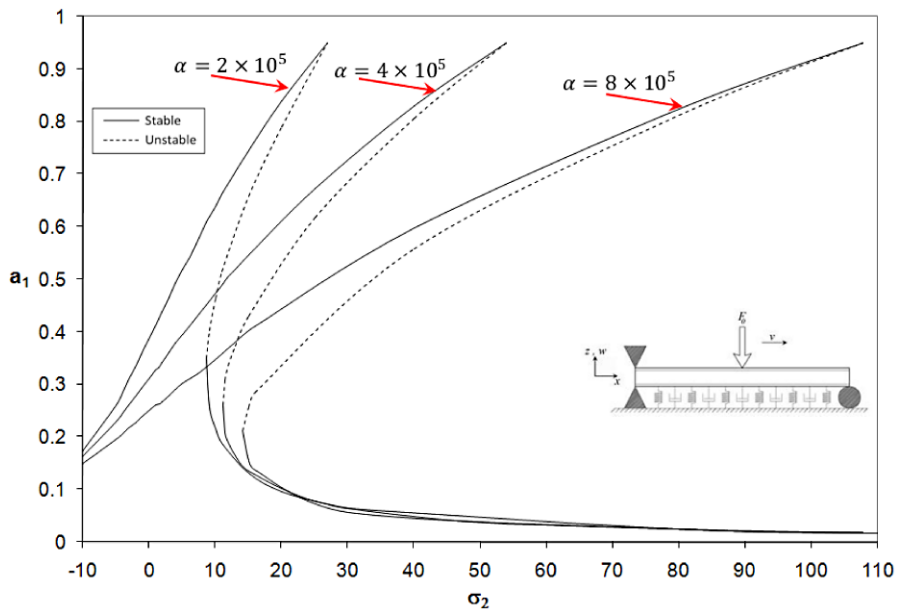

(a)

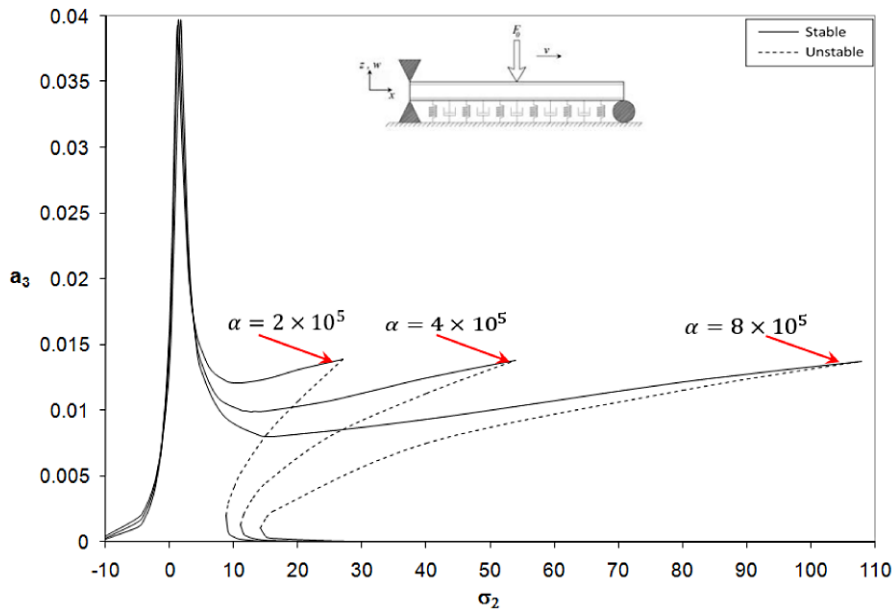

(b)

Fig. 9 (**a**) Effects of nonlinear stiffness on frequency response for a_1 with $\omega_3 \approx 3\omega_1, \Omega_1 \approx \omega_1$. (**b**) Effects of nonlinear stiffness on frequency response for a_3 with $\omega_3 \approx 3\omega_1, \Omega_1 \approx \omega_1$

$$-\frac{3}{8}\alpha_{10}a_3^3 + \omega_3 a_3(3\sigma_2 - \sigma_1) - \frac{1}{4}\alpha_{11}a_1^2 a_3 - \frac{1}{8}\alpha_{14}a_1^3\cos\gamma_1 = 0, \tag{57}$$

$$-\mu a_3\omega_3 + \frac{1}{8}\alpha_{14}a_1^3\sin\gamma_1 = 0 \tag{58}$$

The variations of parameters a_1 and a_3 with σ_2 for three different values of amplitude of the excitation under the condition of $\Omega_1 \approx \omega_1$ are presented in Fig. 7. Furthermore, the effects of the damping coefficient and the non-linear stiffness could be observed from Figs. 8 and 9, respectively.

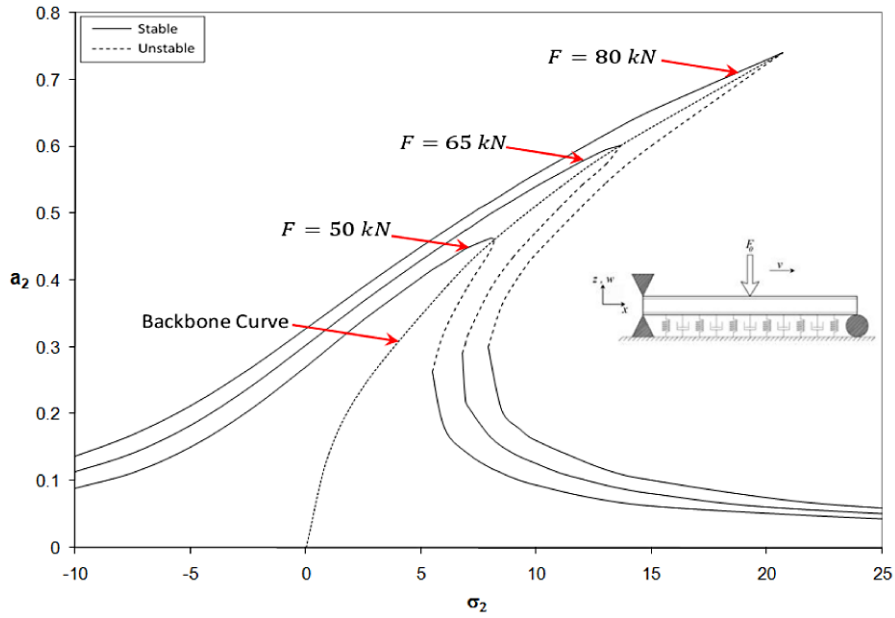

Fig. 10 Frequency response curves when $\omega_3 \approx 3\omega_1, \Omega_2 \approx \omega_2$

3.2.2 Case (b) when $\Omega_2 \approx \omega_2$

In this case, the values of both parameters a_1 and a_3 will be set to zero in accordance with the following equations:

$$a_1\omega_1\theta_1' - \frac{3}{8}\alpha_1 a_1^3 - \frac{1}{4}\alpha_3 a_1 a_2^2 - \frac{1}{4}\alpha_4 a_1 a_3^2 - \frac{1}{8}\alpha_2 a_1^2 a_3 \cos\gamma_1 = 0, \tag{59}$$

$$-\mu a_1\omega_1 - \frac{1}{8}\alpha_2 a_1^2 a_3 \sin\gamma_1 = 0, \tag{60}$$

$$-\frac{1}{4}\alpha_7 a_2 a_1^2 - \frac{1}{4}\alpha_8 a_2 a_3^2 + \omega_2\sigma_2 a_2 - \frac{3}{8}\alpha_6 a_2^3 + \frac{1}{2} f_2 \cos\gamma_2 = 0, \tag{61}$$

$$-\mu a_2\omega_2 + \frac{1}{2} f_2 \sin\gamma_2 = 0, \tag{62}$$

$$-\frac{1}{4}\alpha_{12} a_2^2 a_3 - \frac{3}{8}\alpha_{10} a_3^3 + \omega_3 a_3(3\theta_1' - \sigma_1) - \frac{1}{4}\alpha_{11} a_1^2 a_3 - \frac{1}{8}\alpha_{14} a_1^3 \cos\gamma_1 = 0, \tag{63}$$

$$-\mu a_3\omega_3 + \frac{1}{8}\alpha_{14} a_1^3 \sin\gamma_1 = 0 \tag{64}$$

The variations of parameter a_2 with σ_2, for three different values of the amplitude of excitation under the condition of $\Omega_2 \approx \omega_2$, are illustrated in Fig. 10. The influences of the damping coefficient and the nonlinear stiffness on the frequency-response curves are presented in Figs. 11 and 12, respectively.

3.2.3 Case (c) when $\Omega_3 \approx \omega_3$

In this case by applying the steady-state condition, one may obtain

$$a_2 = 0 \tag{65}$$

Therefore, the following simultaneous equations must be solved.

$$\frac{1}{3}a_1\omega_1(\sigma_1 + \sigma_2) - \frac{3}{8}\alpha_1 a_1^3 - \frac{1}{4}\alpha_4 a_1 a_3^2 - \frac{1}{8}\alpha_2 a_1^2 a_3 \cos\gamma_1 = 0, \tag{66}$$

$$-\mu a_1\omega_1 - \frac{1}{8}\alpha_2 a_1^2 a_3 \sin\gamma_1 = 0, \tag{67}$$

$$-\frac{3}{8}\alpha_{10} a_3^3 + \omega_3 a_3\sigma_2 - \frac{1}{4}\alpha_{11} a_1^2 a_3 - \frac{1}{8}\alpha_{14} a_1^3 \cos\gamma_1 + \frac{1}{2} f_3 \cos\gamma_2 = 0, \tag{68}$$

$$-\mu a_3\omega_3 + \frac{1}{8}\alpha_{14} a_1^3 \sin\gamma_1 + \frac{1}{2} f_3 \sin\gamma_2 = 0 \tag{69}$$

Here, the parameter a_1 is proved to be always zero while a_3 has a non-zero value. The variations of a_3 with σ_2 for three different values of the amplitude of

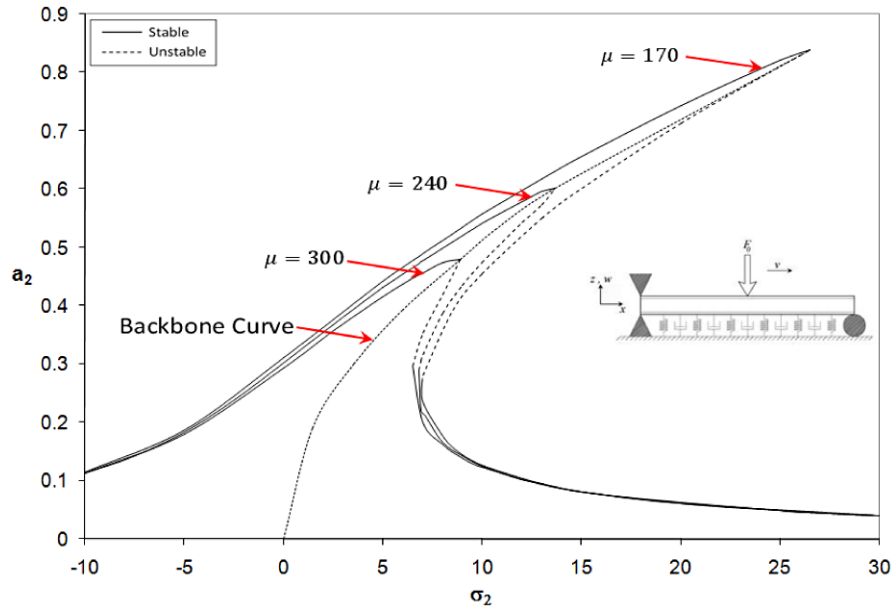

Fig. 11 Effects of damping coefficient on the frequency response curves for $\omega_3 \approx 3\omega_1, \Omega_2 \approx \omega_2$

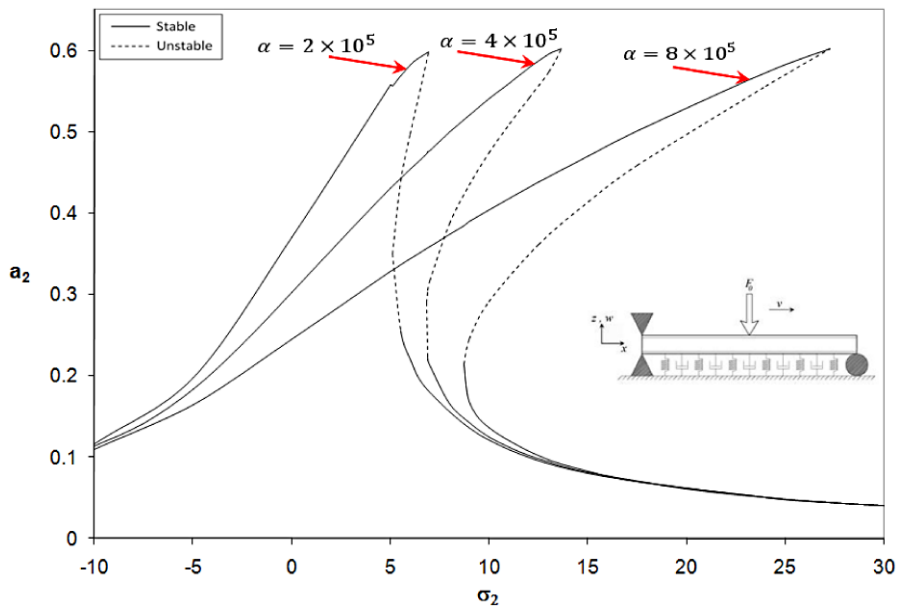

Fig. 12 Effects of nonlinear stiffness on the frequency response curves for $\omega_3 \approx 3\omega_1, \Omega_2 \approx \omega_2$

excitation under the conditions of $\Omega_3 \approx \omega_3$ and $a_1 = 0$ are shown in Fig. 13. The effects of the damping coefficient and the non-linear stiffness parameter on the frequency response curve have been illustrated in Figs. 14 and 15, respectively.

4 Conclusion

Vibration of a finite beam supported by non-linear viscoelastic foundation traversed by a moving load was investigated. The Galerkin method was used to discretize the non-linear partial differential equation of motion and subsequently, its solution was obtained for different harmonics using the multiple scales method (MSM). Free vibration of the beam resting on non-linear foundation was then studied in the case of internal resonance. The effects of damping coefficient and non-linear stiffness of the foundation on the responses were investigated. It was found that the magnitude of the oscillations of the first harmonic is larger

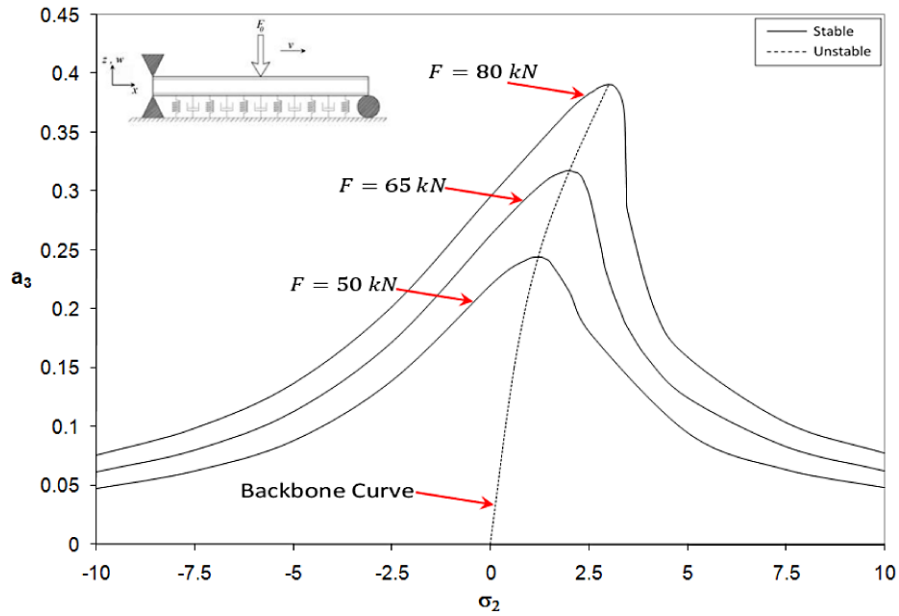

Fig. 13 Frequency response curves for $\omega_3 \approx 3\omega_1, \Omega_3 \approx \omega_3, a_1 = 0$

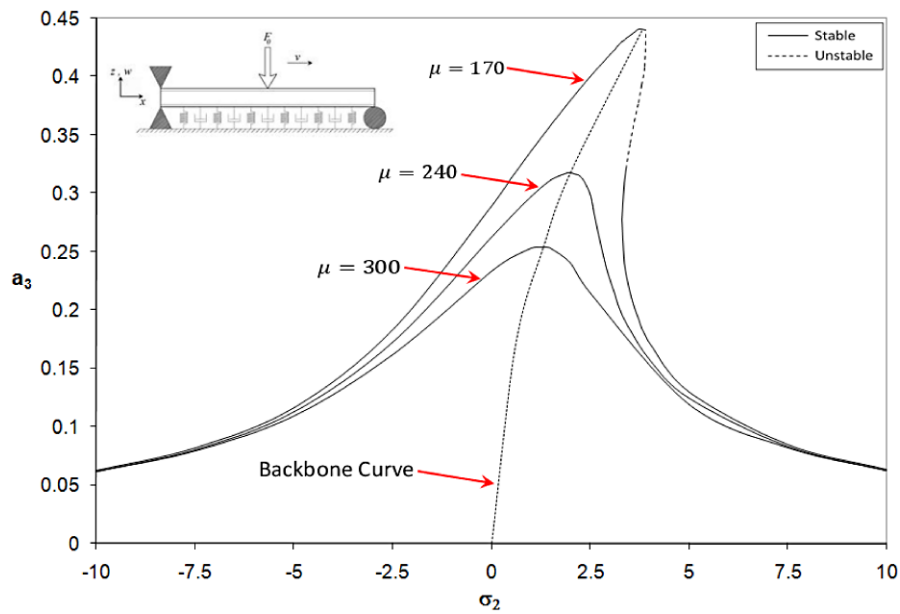

Fig. 14 Effects of damping coefficient on the frequency response curves for $\omega_3 \approx 3\omega_1, \Omega_3 \approx \omega_3, a_1 = 0$

than those of the others and the non-linear stiffness would increase the frequency, as well as the magnitude of vibration, but the rate of dissipation is not affected. The internal-external resonance condition was then considered and the frequency responses of different harmonics were obtained using MSM. Different conditions of external resonance were studied and for each case a parametric sensitivity study was carried out. In the case of moving load, even with a constant magnitude, the jump phenomena will occur in the frequency response. The effects of damping coefficient and non-linear stiffness of the foundation as well as the magnitude of the moving load on the frequency responses were investigated and the backbone curves were obtained for every case. It is found that the sharpness of the frequency responses decrease in the higher order external resonances. In other words, the jump phenomenon will occur at lower detuning parameters.

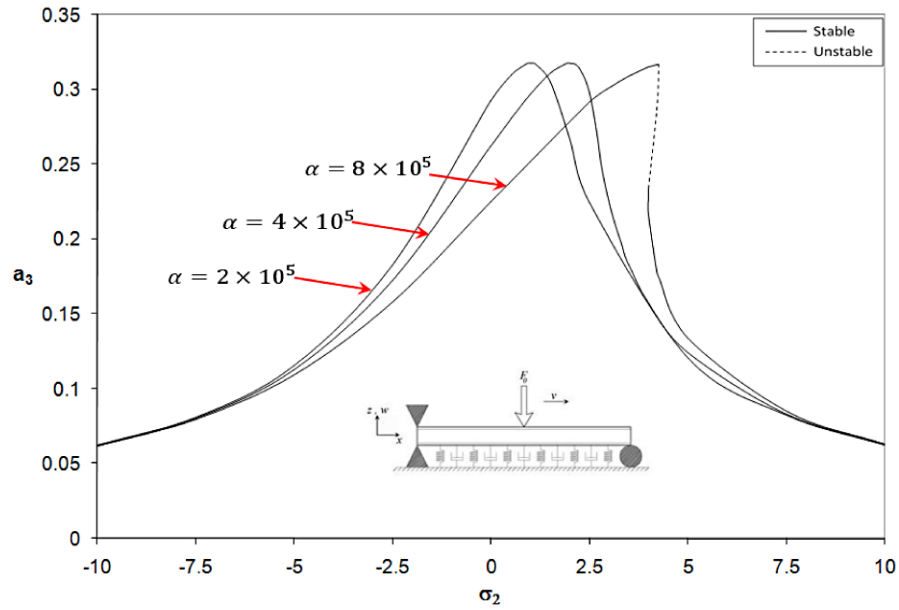

Fig. 15 Effects of nonlinear stiffness on the frequency response curves for $\omega_3 \approx 3\omega_1$, $\Omega_3 \approx \omega_3, a_1 = 0$

In the case of $\omega_3 \approx 3\omega_1, \Omega_1 \approx \omega_1$ a two-branched frequency response was obtained for the third harmonic. Generally, one concludes that all the harmonics are more sensitive to the non-linear stiffness than the damping coefficient or the moving load magnitude. The increase in the damping coefficient and the decrease in the non-linear stiffness can delay the phenomenon of jump more effectively in the lower range of the external resonances.

Acknowledgement The research support provided by the Natural Sciences and Engineering Research Council of Canada (NSERC) to complete this work is greatly appreciated.

Appendix: Example for the stability analysis

The procedure, which was suggested in Sect. 3, will be applied to (31) through (36) in order to demonstrate as how to perform the stability analysis. In this case,

$$\theta_1' = \sigma_2 - \gamma_2', \tag{70}$$

$$\theta_3' = \gamma_1' - 3\gamma_2' + 3\sigma_2 - \sigma_1, \tag{71}$$

$$a_2' = a_2 = 0 \tag{72}$$

Substituting (70) through (72) into (31) through (36), and solving for a_1', a_3', γ_1', and γ_2' one would obtain

$$a_1' = -\mu a_1 - \frac{\alpha_2 a_1^2 a_3 \sin(\gamma_1)}{8\omega_1} + \frac{f_1 \sin(\gamma_2)}{2\omega_1}, \tag{73}$$

$$a_3' = -\mu a_3 + \frac{\alpha_{14} a_1^3 \sin(\gamma_1)}{8\omega_3}, \tag{74}$$

$$\gamma_1' = \frac{3\alpha_{10} a_3^2}{8\omega_3} - \frac{3\alpha_4 a_3^2}{4\omega_1} - \frac{3\alpha_2 a_1 a_3 \cos(\gamma_1)}{8\omega_1} - \frac{9\alpha_1 a_1^2}{8\omega_1} + \frac{3 f_1 \cos(\gamma_2)}{2 a_1 \omega_1} + \sigma_1 + \frac{\alpha_{11} a_1^2}{4\omega_3} + \frac{\alpha_{14} a_1^3 \cos(\gamma_1)}{8\omega_1 a_3}, \tag{75}$$

$$\gamma_2' = \sigma_2 - \frac{\alpha_2 a_1 a_3 \cos(\gamma_1)}{8\omega_1} - \frac{3\alpha_1 a_1^2}{8\omega_1} - \frac{\alpha_4 a_3^2}{4\omega_1} + \frac{f_1 \cos(\gamma_2)}{2 a_1 \omega_1} \tag{76}$$

By linearizing of (73) through (76) and following the instruction given in Sect. 3, one may define the Jacobian matrix as

$$\mathbf{J} = \begin{bmatrix} J_{11} & J_{12} & J_{13} & J_{14} \\ J_{21} & J_{22} & J_{23} & J_{24} \\ J_{31} & J_{32} & J_{33} & J_{34} \\ J_{41} & J_{42} & J_{43} & J_{44} \end{bmatrix} \tag{77}$$

where

$$J_{11} = -\mu - \frac{\alpha_2 a_1 a_3 \sin(\gamma_1)}{4\omega_1}, \tag{78}$$

$$J_{12} = -\frac{\alpha_2 a_1^2 \sin(\gamma_1)}{8\omega_1}, \tag{79}$$

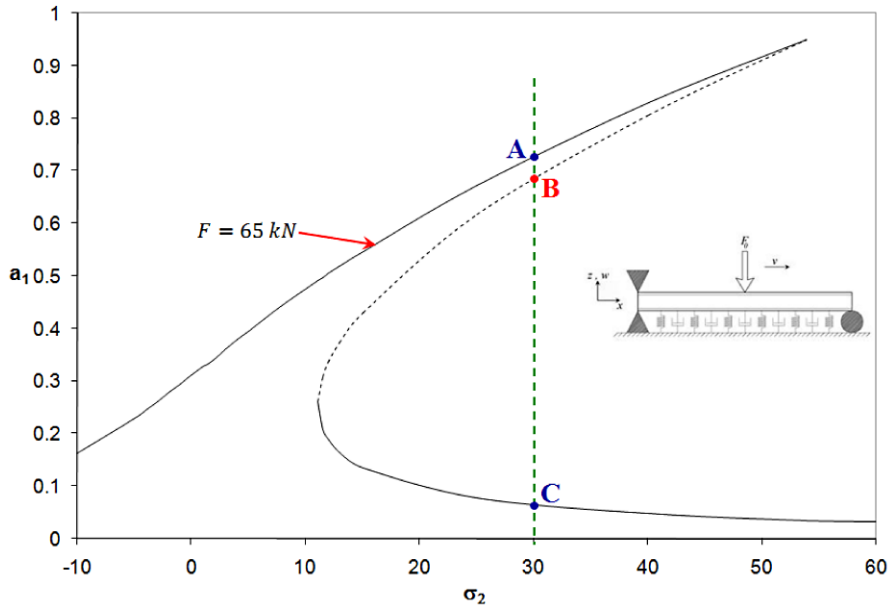

Fig. 16 Frequency response curves for a_1 with $\omega_3 \approx 3\omega_1$, and $\Omega_1 \approx \omega_1$, when $F = 65$ kN

$$J_{13} = -\frac{\alpha_2 a_1^2 a_3 \cos(\gamma_1)}{8\omega_1}, \tag{80}$$

$$J_{14} = \frac{f \sin(\gamma_2)}{2\omega_1}, \tag{81}$$

$$J_{21} = \frac{3\alpha_{14} a_1^2 \sin(\gamma_1)}{8\omega_3}, \tag{82}$$

$$J_{22} = -\mu, \tag{83}$$

$$J_{23} = \frac{\alpha_{14} a_1^3 \cos(\gamma_1)}{8\omega_3}, \tag{84}$$

$$J_{24} = 0, \tag{85}$$

$$J_{31} = -\frac{3\alpha_2 a_3 \cos(\gamma_1)}{8\omega_1} - \frac{9\alpha_1 a_1}{4\omega_1} - \frac{3 f_1 \cos(\gamma_2)}{2a_1^2\omega_1} + \frac{\alpha_{11} a_1}{2\omega_3} + \frac{3\alpha_{14} a_1^2 \cos(\gamma_1)}{8a_3\omega_3}, \tag{86}$$

$$J_{32} = \frac{3\alpha_{10} a_3}{4\omega_3} - \frac{3\alpha_4 a_3}{2\omega_1} - \frac{3\alpha_2 a_1 \cos(\gamma_1)}{8\omega_1} - \frac{\alpha_{14} a_1^3 \cos(\gamma_1)}{8\omega_3 a_3^2}, \tag{87}$$

$$J_{33} = \frac{3\alpha_2 a_1 a_3 \sin(\gamma_1)}{8\omega_1} - \frac{\alpha_{14} a_1^3 \sin(\gamma_1)}{\omega_3 a_3}, \tag{88}$$

$$J_{34} = -\frac{3 f_1 \sin(\gamma_1)}{2a_1\omega_1}, \tag{89}$$

$$J_{41} = -\frac{\alpha_2 a_3 \cos(\gamma_1)}{8\omega_1} - \frac{3\alpha_1 a_1}{4\omega_1} - \frac{f_1 \cos(\gamma_2)}{2\omega_1 a_1^2}, \tag{90}$$

$$J_{42} = -\frac{\alpha_2 a_1 \cos(\gamma_1)}{8\omega_1} - \frac{\alpha_4 a_3}{2\omega_1}, \tag{91}$$

$$J_{43} = \frac{\alpha_2 a_1 a_3 \sin(\gamma_1)}{8\omega_1}, \tag{92}$$

$$J_{44} = \frac{f_1 \sin(\gamma_1)}{2a_1\omega_1}. \tag{93}$$

One particular case in Fig. 7a is considered, as an example, when $F = 65$ kN, and it is illustrated in Fig. 16. If values of different parameters, associated with different points on this graph, are introduced in (77), the Jacobian matrix corresponding to every point would be obtained. Therefore, four eigen-values of this matrix can then be evaluated. If any of the eigen-values have a positive real part, that point will correspond to an unstable performance.

In Fig. 16, all the eigen-values of Jacobian matrices associated with points A and C have negative real parts and, therefore, both of these points represent stable ones. However, if the same numerical analysis is performed for point B, then two of the eigen-values

Table 2 Case studies for stability analysis, corresponding to Fig. 16, where $\sigma_2 = 30$

Points	A	B	C
λ_1	$-1.0966 + 62657.43511i$	$-1.0552 + 64377.7327i$	$-0.9939 + 73870.3654i$
λ_2	$-1.0966 - 62657.43514i$	$-1.0552 - 64377.7327i$	$-0.9939 - 73870.3654i$
λ_3	$-1.9785 + 324.5164i$	$1.9818 + 323.4934i$	$-1.9878 + 134.0352i$
λ_4	$-1.9785 - 324.5164i$	$1.9818 - 323.4934i$	$-1.9878 - 134.0352i$

will have positive real part. Therefore, point B is an unstable one (see Table 2, for the numerical values).

References

1. Fryba, L.: Vibration of Solids and Structures under Moving Loads. Thomas Telford, London (1999)
2. Esmailzadeh, E., Ghorashi, M.: Vibration analysis of Timoshenko beams subjected to a traveling mass. J. Sound Vib. **199**(4), 615–625 (1997)
3. Andersen, L., Nielsen, S.R.K., Kirkegaard, P.H.: Finite element modeling of infinite Euler beams on Kelvin foundations exposed to moving loads in convected co-ordinates. J. Sound Vib. **241**(4), 587–604 (2001)
4. Yu, Y., Nian-Guan, T., Yian-Feng, T.: Vibration analysis of a simply-supported beam traversed by uniform distributed moving loads. J. Shanghai Jiaotong Univ. **38**, 155–160 (2004)
5. Gurav, S.: Dynamic analysis of bridges under moving loads. In: Proceedings, Responding to Tomorrow's Challenges in Structural Engineering, Budapest, Hungary, 13–15 September (2006)
6. Ouyang, H., Mottershead, J.E.: Vibration of a beam excited by a moving flexible body. In: Proceedings, Sixth International Conference on Modern Practice in Stress and Vibration Analysis, Bath, UK, pp. 457–464, 5–7 September (2006)
7. Kim, S.M., Cho, Y.H.: Vibration and dynamic buckling of shear beam-columns on elastic foundation under moving harmonic loads. Int. J. Solids Struct. **43**, 393–412 (2006)
8. Martinez-Castro, A.E., Museros, P., Castillo-Linares, A.: Semi-analytic solution in the time domain for non-uniform multi-span Bernoulli–Euler beams traversed by moving loads. J. Sound Vib. **294**, 278–297 (2006)
9. Garinei, A.: Vibrations of simple beam-like modeled bridge under harmonic moving loads. Int. J. Eng. Sci. **44**, 778–787 (2006)
10. Ouyang, H., Mottershead, J.E.: A numerical-analytical combined method for vibration of a beam excited by a moving flexible body. Int. J. Numer. Methods Eng. **72**, 1181–1191 (2007)
11. Stancioiu, D., Ouyang, H., Mottershead, J.E.: Vibration of a beam excited by a moving oscillator considering separation and reattachment. J. Sound Vib. **310**(4–5), 1128–1140 (2008)
12. Kiral, Z., Goren Kiral, B.: Dynamic analysis of a symmetric laminated composite beam subjected to a moving load with constant velocity. J. Reinf. Plast. Compos. **27**(1), 19–32 (2008)
13. Coskun, I., Engin, H.: Non-linear vibrations of a beam on an elastic foundation. J. Sound Vib. **223**(3), 335–354 (1999)
14. Yanmeni Wayou, A.N., Tchoukuegno, R., Woafo, P.: Non-linear dynamics of an elastic beam under moving loads. J. Sound Vib. **273**(4–5), 1101–1108 (2004)
15. Kang, B., Tan, C.A.: Non-linear response of a beam under distributed moving contact load. Commun. Non-linear Sci. Numer. Simul. **11**, 203–232 (2006)
16. Huang, W., Zou, Y.: The dynamic response of a viscoelastic Winkler foundation-supported elastic beam impacted by a low velocity projectile. Comput. Struct. **52**(3), 431–436 (1994)
17. Ayoub, A.: Mixed formulation of non-linear beam on foundation elements. Comput. Struct. **81**, 411–421 (2003)
18. Patel, B.P., Ganapathi, M., Touratier, M.: Non-linear free flexural vibrations/post-buckling analysis of laminated orthotropic beams/columns on a two parameter elastic foundation. Compos. Struct. **46**, 189–196 (1999)
19. Naidu, N.R., Rao, G.V.: Free vibration and stability behavior of uniform beams and columns on non-linear elastic foundation. Comput. Struct. **58**(6), 1213–1215 (1996)
20. Lenci, S., Tarantino, A.M.: Chaotic dynamics of an elastic beam resting on a Winkler-type soil. Chaos Solitons Fractals **7**(10), 1601–1614 (1996)
21. Coskun, I.: The response of a finite beam on a tensionless Pasternak foundation subject to a harmonic load. Eur. J. Mech. A/Solids **22**, 151–161 (2003)
22. Sheinman, I., Adan, M., Altus, E.: On the role of the displacement function in non-linear analysis of beams on an elastic foundation. Thin-Walled Struct. **15**(2), 109–125 (1993)
23. Kuo, Y.H., Lee, S.Y.: Deflection of non-uniform beams resting on a non-linear elastic foundation. Comput. Struct. **51**(5), 513–519 (1994)
24. Santee, D.M., Goncalves, P.B.: Oscillations of a beam on a non-linear elastic foundation under periodic loads. Shock Vib. **13**, 273–284 (2006)
25. Dahlberg, T.: Dynamic interaction between train and non-linear railway track model. In: Proceedings, Fifth European Conference on Structural Dynamics (EURODYN 2002), Munich, Germany, vol. 2, pp. 1155–1160, 2–5 September (2002)

26. Kargarnovin, M.H., Younesian, D., Thompson, D.J., Jones, C.J.C.: Response of beams on non-linear viscoelastic foundations to harmonic moving loads. Comput. Struct. **83**, 1865–1877 (2005)
27. Nayfeh, A.H., Mook, D.T.: Nonlinear Oscillations. Wiley, New York (1979)
28. Abe, A.: On non-linear vibration analyses of continuous systems with quadratic and cubic non-linearities. Int. J. Non-Linear Mech. **41**, 873–879 (2006)
29. Iwnicky, S.: Handbook of Railway Vehicle Dynamics. Taylor and Francis, New York (2007)
30. Wu, T.X., Thompson, D.J.: The effects of track nonlinearity on wheel/rail impact. Proc. Inst. Mech. Eng., F., J. Rail Rapid Transit **218**(1), 1–15 (2004)